



Robust receiver for OFDM-DCSK modulation via rank-1 modeling and ℓ_p -minimization

Zhaofeng Liu^a, Hing Cheung So^{a,*}, Lin Zhang^b, Xiao Peng Li^a

^a Department of Electrical Engineering, City University of Hong Kong, Kowloon Tong, Hong Kong

^b School of Electronics and Information Technology, Sun Yat-sen University, Guangzhou, China

ARTICLE INFO

Article history:

Received 22 December 2020

Revised 11 May 2021

Accepted 18 June 2021

Available online 27 June 2021

Keywords:

Bit error rate

Differential chaos shift keying

ℓ_p -minimization

Impulsive noise

ABSTRACT

In this paper, the problem of receiver design for orthogonal frequency division multiplexing differential chaos shift keying (OFDM-DCSK) communication systems is addressed. By exploiting the rank-1 property of the symbol matrix, we propose to apply dimensionality reduction on the time-domain data symbols received from the OFDM-DCSK transmitter for noise reduction, followed by chaotic demodulation on the resultant symbols to decode the information bits. In the presence of additive white Gaussian noise (AWGN), the rank-1 matrix approximation can be simply achieved by the truncated singular value decomposition, corresponding to the solution of ℓ_2 -norm minimization. While for impulsive noise environments such as in power line communication systems, we develop an alternating optimization algorithm for ℓ_p -based matrix factorization, where $0 < p < 2$. The bit error rate (BER) of our approach in AWGN is also analyzed and verified. Simulation results demonstrate that the devised receiver is superior to the conventional OFDM-DCSK method in terms of BER and root mean square error performance for AWGN as well as impulsive noise including the Middleton class A distribution and α -stable process.

© 2021 Elsevier B.V. All rights reserved.

1. Introduction

Nowadays, wireless communication systems are easily eavesdropped by malicious users due to channel broadcast characteristics and lack of encryption. In order to enhance their security, chaotic communication is one of the effective encryption schemes [1] for data transmission in ultra-wide-band (UWB) and power line communication (PLC) systems [2] because the chaotic sequences have naturally high-security properties including noise-like feature, sensitivity to the initial value and good auto-correlation [3]. Among different chaotic techniques, coherent or non-coherent chaotic modulation has attracted considerable attention in the literature. In particular, non-coherent chaotic modulation [4] is widely discussed for removing complex chaotic synchronization modules.

Differential chaos shift keying (DCSK) [4] is one of the most practical non-coherent chaotic modulation schemes since it performs the non-coherent demodulation on the reference sequence and information-bearing sequences, and the receiver does not need to generate the chaotic waveform. Moreover, it can provide a satisfactory bit error rate (BER) performance for UWB and PLC communication systems [1]. However, DCSK has two main drawbacks,

namely, low transmission efficiency and the requirement of highly-complex delay line circuits [1].

To simultaneously address these two issues, multi-carrier (MC) based DCSK system has been suggested [5]. In MC-DCSK, one subcarrier is assigned for the reference sequence transmission while the remaining subcarriers are allocated for transmitting information-bearing sequences. Since different sequences are located in different subcarriers, the delay line circuit is not needed. Moreover, the number of subcarriers can be sufficiently large, thereby the transmission efficiency is significantly enhanced. In addition, the orthogonal frequency division multiplexing (OFDM) technique can be applied in MC-DCSK systems to reduce the implementation complexity. The resultant OFDM-DCSK system [6] is easily realized by fast Fourier transform (FFT), and can utilize the spectrum more efficiently than the MC-DCSK system, resulting in higher transmission efficiency. The OFDM-DCSK has also been extended to the multiuser scenarios in Kaddoum [7], while [8,9] focus on further improving the security performance.

On the other hand, although DCSK has been applied in PLC systems, the impulsive noise together with Gaussian noise in these channels [10,11] can remarkably degrade the BER performance. In particular, the former induces large-amplitude disturbance or outliers to the transmitted chaotic sequences, which will introduce many erroneous data after non-coherent demodulation at the receiver. In the presence of Gaussian noise, Kaddoum and Soujeri

* Corresponding author.

E-mail addresses: zhaofeliu3-c@my.cityu.edu.hk (Z. Liu), hcsso@ee.cityu.edu.hk (H. Cheung So), isszl@mail.sysu.edu.cn (L. Zhang), x.p.li@my.cityu.edu.hk (X.P. Li).

[12] has adopted the DCSK scheme with repeatedly transmitted reference sequence and moving average filter at the receiver for noise reduction. In addition, Rao et al. [13] has proposed an iterative chaos generator with average computation at the receiver. While in Chen et al. [14], an iterative MC-DCSK receiver is developed for increasing the reference sequence accuracy. However, they all have not considered handling the outlier-contaminated data. Miao et al. [15] has suggested an M -ary DCSK system with replica piecewise frame to reduce the impulsive noise. However, it is only focused on DCSK systems in the time domain, and hence cannot utilize the MC structure to enhance transmission efficiency.

In this work, we exploit the fact that all information-bearing sequences are generated by multiplying the reference sequence by a scalar to enhance the receiver design. That is, since every chaotic sequence in an OFDM-DCSK symbol can be viewed as a row in a matrix, we propose to model the transmitted OFDM-DCSK signal as a rank-1 matrix, and then perform rank-1 matrix approximation based detection at the receiver for noise reduction. To the best of our knowledge, this idea has not yet been initiated in the literature. It is worth mentioning that low-rank matrix approximation can be simply realized by the truncated singular value decomposition (SVD), which corresponds to least squares (LS) or ℓ_2 -norm minimization, yielding the optimum receiver for Gaussian noise suppression [16]. Nevertheless, the LS approach may result in degraded performance for impulsive noise because the squaring operator in the ℓ_2 -norm will notably amplify the large-amplitude outlier components, making it not robust to outliers. A conventional outlier-resistant solution is to generalize the ℓ_2 -norm to ℓ_p -norm, where $0 < p \leq 2$ [17]. That is because when $p < 2$, the impulsive noise is not amplified too much during the ℓ_p -minimization, resulting in that the large residuals caused by the outliers are smaller and not dominating the optimization process. In fact, ℓ_p -norm based minimization for matrix approximation has wide applicability such as robust direction-of-arrival estimation [18] and image painting [19].

Our main contributions are summarized as:

1. By exploiting the rank-1 property of the transmission matrix, a novel idea is devised in the OFDM-DCSK receiver design by integrating a low-rank matrix approximation procedure in the system to achieve noise reduction, which in turn lowers the BER.
2. We propose to use the matrix factorization technique to estimate the resultant rank-1 matrix where the ℓ_p -minimization problem formulation is adopted. For $0 < p < 2$, the receiver is robust even to the impulsive noise, and the solver is realized based on alternating optimization. The algorithm local/global convergence is also proved. While for $p = 2$, it is basically an LS problem and the solution is simply computed by the truncated SVD, but this may not provide reliable performance in the presence of outlier-contaminated data. It is shown that our low-rank approximation approach significantly outperforms [6] in both BER and mean square error metrics.
3. We derive the BER expression for the proposed rank-1 approximation OFDM-DCSK receiver in AWGN, which is validated via computer simulations.

The rest of this paper is organized as follows. Section 2 describes our OFDM-DCSK system, which consists of the rank-1 matrix approximation step via ℓ_p -minimization in the receiver. The solvers for $p = 2$ and $0 < p < 2$ are developed. The latter is based on alternating minimization and we also study the algorithm convergence. In Section 3, the BER of the proposed receiver in the presence of AWGN is derived. Section 4 presents the evaluation results of the rank-1 approximation approach in AWGN as well as impulsive noise, namely, Middleton class A distribution and α -

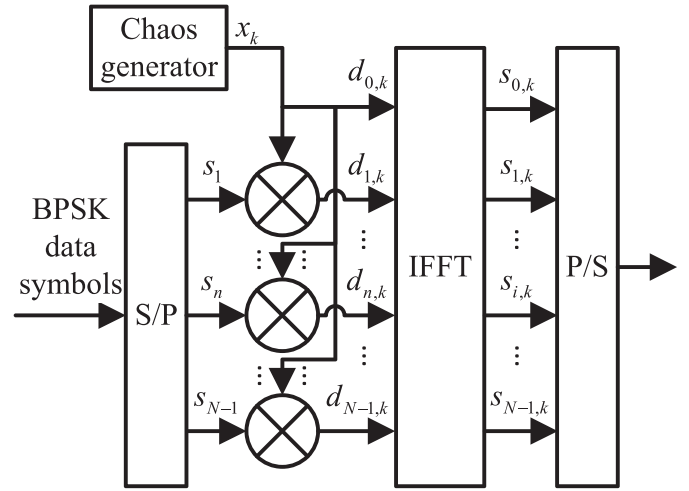


Fig. 1. Block diagram of OFDM-DCSK transmitter.

stable process, for different values of p and signal-to-noise ratio conditions. Finally, conclusions are drawn in Section 5.

2. Rank-1 approximation based OFDM-DCSK design

In this section, we present our proposed OFDM-DCSK system where the novelty lies in the rank-1 approximation design in the receiver.

2.1. Transmitter structure

Fig. 1 depicts the block diagram of a standard OFDM-DCSK transmitter [6]. The information from users is firstly modulated as binary phase shift keying (BPSK) data symbols. After serial-to-parallel (S/P) conversion, they are multiplied by the reference chaotic sequence $\{x_k\}$ where $x_k \in (-1, 0) \cup (0, 1)$ is the k th chip generated by the second-order Chebyshev polynomial function (CPF) chaos generator according to $x_{k+1} = 1 - 2x_k^2$, $0 \leq k \leq \beta - 1$, with β being the sequence length. The k th chip of the chaotic modulated sequence in the n th data stream can be expressed as $d_{n,k} = s_n x_k$, $1 \leq n \leq N - 1$ while the k th chip of the reference chaotic sequence is also represented as $d_{0,k} = x_k$ since $s_0 = 1$. Subsequently, one reference and $N - 1$ chaotic modulated sequences are sent to the inverse FFT (IFFT) module to perform OFDM modulation. The resultant symbols, expressed as $s_{i,k} = \sum_{n=0}^{N-1} d_{n,k} e^{j2\pi ni/N} / \sqrt{N}$, $i = 0, \dots, N - 1$, $k = 0, \dots, \beta - 1$, then go through parallel-to-serial (P/S) conversion, prior to transmitting over a wireless channel.

Define $\mathbf{S} \in \mathbb{C}^{N \times \beta}$, whose entries are $\{s_{i,k}\}$, it can be factorized as:

$$\mathbf{S} = \mathbf{p}\mathbf{x}^T = [\mathbf{s}_0, \mathbf{s}_1, \dots, \mathbf{s}_k, \dots, \mathbf{s}_{\beta-1}]$$

$$= \begin{bmatrix} p_0 x_0 & p_0 x_1 & \dots & p_0 x_k & \dots & p_0 x_{\beta-1} \\ p_1 x_0 & p_1 x_1 & \dots & p_1 x_k & \dots & p_1 x_{\beta-1} \\ \vdots & \vdots & \ddots & \vdots & \ddots & \vdots \\ p_i x_0 & p_i x_1 & \dots & p_i x_k & \dots & p_i x_{\beta-1} \\ \vdots & \vdots & \ddots & \vdots & \ddots & \vdots \\ p_{N-1} x_0 & p_{N-1} x_1 & \dots & p_{N-1} x_k & \dots & p_{N-1} x_{\beta-1} \end{bmatrix} \quad (1)$$

where $\mathbf{s}_k = [s_{0,k}, s_{1,k}, \dots, s_{i,k}, \dots, s_{N-1,k}]^T$, $(\cdot)^T$ is the transpose, $s_{i,k} = p_i x_k$, $\mathbf{p} = [p_0, p_1, \dots, p_n, \dots, p_{N-1}]^T$ is the resultant vector after performing IFFT on $[s_0, s_1, \dots, s_n, \dots, s_{N-1}]^T$, and $\mathbf{x} = [x_0, x_1, \dots, x_k, \dots, x_{\beta-1}]^T$. Apparently, the rank of \mathbf{S} is 1, and this property is exploited in the receiver design.

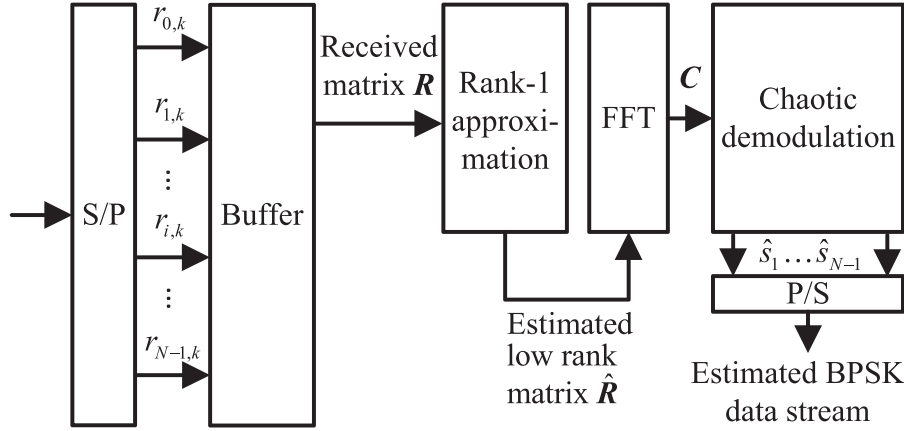


Fig. 2. Block diagram of OFDM-DCSK receiver via rank-1 modeling and ℓ_p -minimization.

2.2. Receiver structure

Fig. 2 illustrates the proposed rank-1 approximation based OFDM-DCSK receiver via ℓ_p -minimization, $0 < p \leq 2$. After the S/P conversion, the received β symbols in N data streams are stored in a buffer, then releasing a matrix $\mathbf{R} \in \mathbb{C}^{N \times \beta}$, which can be expressed as:

$$\mathbf{R} = \mathbf{H}\mathbf{S} + \mathbf{N} \quad (2)$$

where $\mathbf{H} \in \mathbb{C}^{N \times N}$ is a Toeplitz matrix representing the channel effect and $\mathbf{N} \in \mathbb{C}^{N \times \beta}$ is the additive noise matrix. Here the wireless channel response is assumed stationary in an OFDM-DCSK transmission frame and known at the receiver [8]. For presentation simplicity but without loss of generality, we assume that perfect equalization has been performed prior to the S/P conversion, hence $\mathbf{H} = \mathbf{I}$, where \mathbf{I} is the identity matrix.

In the devised rank-1 approximation step in the time domain, we aim to find $\hat{\mathbf{R}} \in \mathbb{C}^{N \times \beta}$ such that $\hat{\mathbf{R}} = \mathbf{u}\mathbf{v}^H$ where $\mathbf{u} \in \mathbb{C}^N$, $\mathbf{v} \in \mathbb{C}^\beta$ and $(\cdot)^H$ is the Hermitian transpose, from \mathbf{R} by utilizing the rank-1 property of \mathbf{S} . In the presence of AWGN, the optimum solution is determined from:

$$\min_{\mathbf{u}, \mathbf{v}} \|\mathbf{u}\mathbf{v}^H - \mathbf{R}\|_F^2 \quad (3)$$

where $\|\cdot\|_F$ is the Frobenius norm. According to the Eckart-Young-Mirsky theorem, it is well known that the solution is:

$$\hat{\mathbf{R}} = \sigma_1 \mathbf{g}\mathbf{h}^H \quad (4)$$

where σ_1 is the largest singular value in the SVD of \mathbf{R} while \mathbf{g} and \mathbf{h} are the associated left and right singular vectors.

For impulsive noise, the truncated SVD is not able to compute a reliable $\hat{\mathbf{R}}$ because the ℓ_2 -minimization is sensitive to outliers. To attain robust performance, we generalize the estimation of $\hat{\mathbf{R}}$ via ℓ_p -minimization, $0 < p \leq 2$ [17]:

$$\min_{\mathbf{u}, \mathbf{v}} \|\mathbf{u}\mathbf{v}^H - \mathbf{R}\|_p^p \quad (5)$$

where $\|\cdot\|_p$ is the element-wise matrix ℓ_p -norm, defined as:

$$\|\mathbf{E}\|_p = \|\mathbf{u}\mathbf{v}^H - \mathbf{R}\|_p = \left(\sum_{n,k} |e_{n,k}|^p \right)^{1/p} \quad (6)$$

with $e_{n,k}$ being the (n, k) entry of \mathbf{E} . Following the idea of [17], \mathbf{u} and \mathbf{v} are iteratively updated via alternating optimization:

$$\mathbf{v}^{l+1} = \arg \min_{\mathbf{v}} \|\mathbf{u}^l \mathbf{v}^H - \mathbf{R}\|_p^p \quad (7)$$

$$\mathbf{u}^{l+1} = \arg \min_{\mathbf{u}} \|\mathbf{u} (\mathbf{v}^{l+1})^H - \mathbf{R}\|_p^p \quad (8)$$

where l corresponds to the estimate at the l th iteration. As the elements in \mathbf{v}^{l+1} or \mathbf{u}^{l+1} are independent in the minimization process, we propose determining them in an entry-by-entry manner:

$$\mathbf{v}_k^{l+1} = \arg \min_{v_k} \|\mathbf{u}^l \mathbf{v}_k - \mathbf{r}_k\|_p^p \quad (9)$$

$$\mathbf{u}_n^{l+1} = \arg \min_{u_n} \|u_n (\mathbf{v}^{l+1})^H - (\tilde{\mathbf{r}}_n)^H\|_p^p \quad (10)$$

where \mathbf{v}_k^{l+1} is the k th element of \mathbf{v}^{l+1} , \mathbf{r}_k is the k th column of \mathbf{R} , \mathbf{u}_n^{l+1} is the n th element of \mathbf{u}^{l+1} and $(\tilde{\mathbf{r}}_n)^H$ is the n th row of \mathbf{R} . One standard solver for (9) and (10) is the iteratively reweighted least squares (IRLS) algorithm [20,21], and the iterative solutions are computed until convergence:

$$\mathbf{v}_k^{q+1} = \arg \min_{v_k} \|\mathbf{W}_N^q (\mathbf{u}^l \mathbf{v}_k - \mathbf{r}_k)\|_p^p \quad (11)$$

$$\mathbf{u}_n^{q+1} = \arg \min_{u_n} \|(u_n (\mathbf{v}^{l+1})^H - (\tilde{\mathbf{r}}_n)^H) \tilde{\mathbf{W}}_\beta^q\|_p^p \quad (12)$$

where q is the inner iteration number, \mathbf{W}_N^q and $\tilde{\mathbf{W}}_\beta^q$ are diagonal matrices whose (n, n) and (k, k) entries are $w_n^q = |\xi_n^q|^{p/2-1}$ and $\tilde{w}_k^q = |\tilde{\xi}_k^q|^{p/2-1}$, respectively, with ξ_n^q and $\tilde{\xi}_k^q$ being the n th and k th entries of $\xi^q = \mathbf{u}^l \mathbf{v}_k - \mathbf{r}_k$ and $\tilde{\xi}^q = u_n (\mathbf{v}^{l+1})^H - (\tilde{\mathbf{r}}_n)^H$. The ℓ_p -minimization procedure is summarized in Algorithm 1. When $1 \leq p < 2$, the IRLS algorithm provides global convergence since the problem is convex, while $0 < p < 1$, the algorithm only has local

Algorithm 1 ℓ_p -minimization for OFDM-DCSK receiver.

Input: \mathbf{R} , p

if $p = 2$ **then**

 Perform truncated SVD on \mathbf{R} to compute $\hat{\mathbf{R}}$ according to (4).

else

Initialize: Randomly initialize all entries in \mathbf{u}^0 as ± 1 .

for $l = 0, 1, \dots$ **do**

for $k = 0, 1, \dots, \beta - 1$ **do**

 Update \mathbf{v}_k^{l+1} based on (9).

end for

for $n = 0, 1, \dots, N - 1$ **do**

 Update \mathbf{u}_n^{l+1} based on (10).

end for

Stop when termination condition is met.

end for

$\hat{\mathbf{R}} = \mathbf{u}^{l+1} (\mathbf{v}^{l+1})^H$.

end if

Output: $\hat{\mathbf{R}}$

convergence. The proof for convergence is provided by the following proposition [18].

Proposition 1. Define the residual error after the l th iteration as $J_p(\mathbf{u}^l, \mathbf{v}^l) = \|\mathbf{u}^l(\mathbf{v}^l)^H - \mathbf{R}\|_F^p$, $J_p(\mathbf{u}^l, \mathbf{v}^l)$ is non-increasing in the iterative process and finally converges to a limit.

Proof. According to (7) and (8), the residual error has the following property:

$$J_p(\mathbf{u}^{l+1}, \mathbf{v}^{l+1}) \leq J_p(\mathbf{u}^l, \mathbf{v}^{l+1}) \leq J_p(\mathbf{u}^l, \mathbf{v}^l). \quad (13)$$

This means that the error will not increase during each iteration. Moreover, the error has a lower bound of 0, thereby the algorithm converges [18]. \square

Following [17], the complexity of Algorithm 1 is $\mathcal{O}(N\beta N_{\text{IRLS}})$ where N_{IRLS} is the required iteration number for convergence. When $p = 2$, the algorithm can be efficiently solved by the truncated SVD, thus $N_{\text{IRLS}} = 1$ and the complexity is reduced to $\mathcal{O}(N\beta)$. In our study, when the absolute difference of normalized root mean square error (NRMSE) between two successive iterations is smaller than $\epsilon = 10^{-4}$, then the algorithm is terminated or convergence condition is reached. The NRMSE is defined as:

$$\text{NRMSE} = \frac{\|\hat{\mathbf{R}} - \mathbf{S}\|_F}{\|\mathbf{S}\|_F} \quad (14)$$

which measures the closeness between the time-domain rank-1 $\hat{\mathbf{R}}$ and \mathbf{S} .

After rank-1 approximation, FFT is applied on $\hat{\mathbf{R}}$ for OFDM demodulation to generate a rank-1 matrix \mathbf{C} . Note that every row vector of \mathbf{C} represents a chaotic sequence, we write \mathbf{C} as:

$$\mathbf{C} = [\mathbf{c}_0, \mathbf{c}_1, \dots, \mathbf{c}_n, \dots, \mathbf{c}_{N+1}]^H \quad (15)$$

where $\mathbf{c}_n \in \mathbb{C}^\beta$ is the n th chaotic sequence and $\mathbf{c}_0 \in \mathbb{C}^\beta$ is the reference sequence. Since the ideal \mathbf{C} must be real, the demodulated BPSK symbol \hat{s}_n is obtained by the following chaotic demodulation:

$$\hat{s}_n = \text{sgn}(\Re\{\mathbf{c}_0\}^T \cdot \Re\{\mathbf{c}_n\}), \quad 1 \leq n \leq N - 1 \quad (16)$$

where $\Re\{\cdot\}$ takes the real part of a complex number and $\text{sgn}(\cdot)$ is the sign function. Finally, the information bits are obtained from \hat{s}_n thanks to the BPSK-symbol decoding.

3. Bit error rate analysis

In this section, we study the BER performance of the proposed receiver over AWGN channel. First, we write $\Re\{\mathbf{C}\} \approx \tilde{\mathbf{u}}\tilde{\mathbf{v}}^T$ where $\tilde{\mathbf{u}} = [\tilde{u}_0, \tilde{u}_1, \dots, \tilde{u}_n, \dots, \tilde{u}_{N-1}]^T \in \mathbb{R}^N$ and $\tilde{\mathbf{v}} \in \mathbb{R}^\beta$ are unique up to a scalar, and interpret the rank-1 approximation as projecting the received noisy sequence onto $\tilde{\mathbf{v}}$. $\tilde{\mathbf{v}}$ is approximately equal to the chaotic sequence \mathbf{x} , and $\tilde{u}_n\tilde{\mathbf{v}}$ is the projection of noisy sequences onto $\tilde{\mathbf{v}}$. Note that $\tilde{\mathbf{v}}^T\tilde{\mathbf{v}} > 0$, (16) can then be expressed as:

$$\begin{aligned} \hat{s}_n &= \text{sgn}(\Re\{\mathbf{c}_0\}^T \cdot \Re\{\mathbf{c}_n\}) = \text{sgn}((\tilde{u}_0\tilde{\mathbf{v}})^T(\tilde{u}_n\tilde{\mathbf{v}})) \\ &= \text{sgn}((\tilde{u}_0\tilde{u}_n)(\tilde{\mathbf{v}}^T\tilde{\mathbf{v}})) = \text{sgn}(\tilde{u}_0) \cdot \text{sgn}(\tilde{u}_n) \end{aligned} \quad (17)$$

whose value is determined by the signs of \tilde{u}_0 and \tilde{u}_n .

Considering that s_n are equally distributed as $+1$ and -1 , we define the error probability P_b of \tilde{u}_n as $P_b = P_b|s_n = +1 = Q(d_{\mathbf{x}\tilde{\mathbf{v}}}/\sigma)$, where $Q(\cdot)$ is the Q-function defined as $Q(x) = \int_x^\infty e^{-t^2/2} dt$, $d_{\mathbf{x}\tilde{\mathbf{v}}}$ is the projection length of \mathbf{x} onto $\tilde{\mathbf{v}}$, which is also equal to the distance between \mathbf{x} and the hyperplane dividing the sign of \tilde{u}_n in the β -dimensional space, and $\sigma = \sqrt{N_0/2}$ is the standard deviation of the AWGN, with N_0 being the noise power spectral density. An illustration for the 2-D case is provided in Fig. 3 and it shows that $\tilde{\mathbf{v}}$ is perpendicular to the hyperplane. Since the

origin is contained in the hyperplane, $d_{\mathbf{x}\tilde{\mathbf{v}}}$ can be determined by the length $d_{\mathbf{x}}$ of \mathbf{x} and the phase θ between \mathbf{x} and $\tilde{\mathbf{v}}$:

$$d_{\mathbf{x}\tilde{\mathbf{v}}} = d_{\mathbf{x}} \cos \theta = \sqrt{\beta} \mathbb{E}\{x_k^2\} \cos \theta = \sqrt{\frac{\beta}{2}} \left| \frac{\tilde{\mathbf{v}}^T \mathbf{x}}{\|\tilde{\mathbf{v}}\|_2 \|\mathbf{x}\|_2} \right| \quad (18)$$

where $\mathbb{E}\{x_k^2\} = 1/2$ since the chaos generator uses the second-order CPF [22], and $\cos \theta = |\tilde{\mathbf{v}}^T \mathbf{x}| / (\|\tilde{\mathbf{v}}\|_2 \|\mathbf{x}\|_2) \geq 0$, implying that $\theta \in [-\pi/2, \pi/2]$. Therefore, P_b is calculated as:

$$P_b = Q\left(\frac{d_{\mathbf{x}\tilde{\mathbf{v}}}}{\sigma}\right) = Q\left(\cos \theta \sqrt{\frac{\beta/2}{N_0/2}}\right) = Q\left(\cos \theta \sqrt{\frac{\beta}{N_0}}\right). \quad (19)$$

The error probability of the BPSK symbols $\{\hat{s}_n\}$ can be computed using P_b . According to (17), since the demodulation is non-coherent, \hat{s}_n is erroneous when either $\text{sgn}(\tilde{u}_0)$ or $\text{sgn}(\tilde{u}_n)$ is incorrect. While if both \tilde{u}_0 and \tilde{u}_n are of wrong signs, the demodulated \hat{s}_n is still correct. Therefore, we can write the error probability P_e of \hat{s}_n as:

$$P_e = 2P_b(1 - P_b). \quad (20)$$

Finally, as θ is randomly distributed, the BER is the expected value of P_e over θ [23]:

$$\begin{aligned} \text{BER} &= \mathbb{E}\{P_e|\theta\} \\ &= \mathbb{E}\left\{2Q\left(\cos \theta \sqrt{\frac{\beta}{N_0}}\right) \left(1 - Q\left(\cos \theta \sqrt{\frac{\beta}{N_0}}\right)\right) \middle| \theta\right\} \end{aligned} \quad (21)$$

which can be numerically evaluated. Note that (21) is applicable for the AWGN because its transform from time domain to frequency domain via FFT is also AWGN, but it is not true for impulsive noise models.

4. Simulation results

Numerical simulations are conducted to evaluate the BER and NRMSE performance of the proposed receiver with comparison to the conventional OFDM-DCSK system where there is no rank-1 approximation procedure [6]. Second-order CPF is considered and the energy used for transmitting a bit is $E_b = N\beta \mathbb{E}\{x_k^2\} / (N - 1)$ where we set $N = 128$ and $\beta = 50$.

First, the BERs of the proposed receiver and [6] in the presence of complex-valued circular AWGN are investigated with respect to E_b/N_0 , which is the signal-to-noise ratio per bit, and the results are shown in Fig. 4. The power of the AWGN is varied to produce $E_b/N_0 \in [-20, 15]$ dB, and for each E_b/N_0 sample point, we perform 3938 independent runs corresponding to $3938 * (N - 1) \approx 500,000$ bits. In simulating the multipath fading channel, the number of paths is 3, with path delay symbols of 0, 2, 4, and the average power of each path is 1/3. The theoretical BER is determined from (21). It is seen that our scheme achieves a much lower BER than [6] for all values of p , with $p = 2$ being the best. It is because the ℓ_2 -norm is regarded as the optimum receiver over AWGN channel [16]. While for $1 \leq p < 2$, its BER performance is comparable to that of $p = 2$, demonstrating the robustness of ℓ_p -norm minimization. Note that the BER results for $p < 1$ are inferior which might be due to the algorithm local convergence. We also find that the theoretical calculation of (21) agrees well with the empirical curve at $p = 2$. In Fig. 5, the BER performance over multipath fading channel is similar to that over AWGN channel with the best performance at $p = 2$. The corresponding NRMSEs are plotted in Fig. 6, which align with Fig. 4, and it is observed that our proposed receiver has smaller NRMSE values than [6].

The above test is then repeated with an impulsive noise channel. We start with the Middleton class A noise which is based on the Gaussian mixture model [24]. Its probability density function

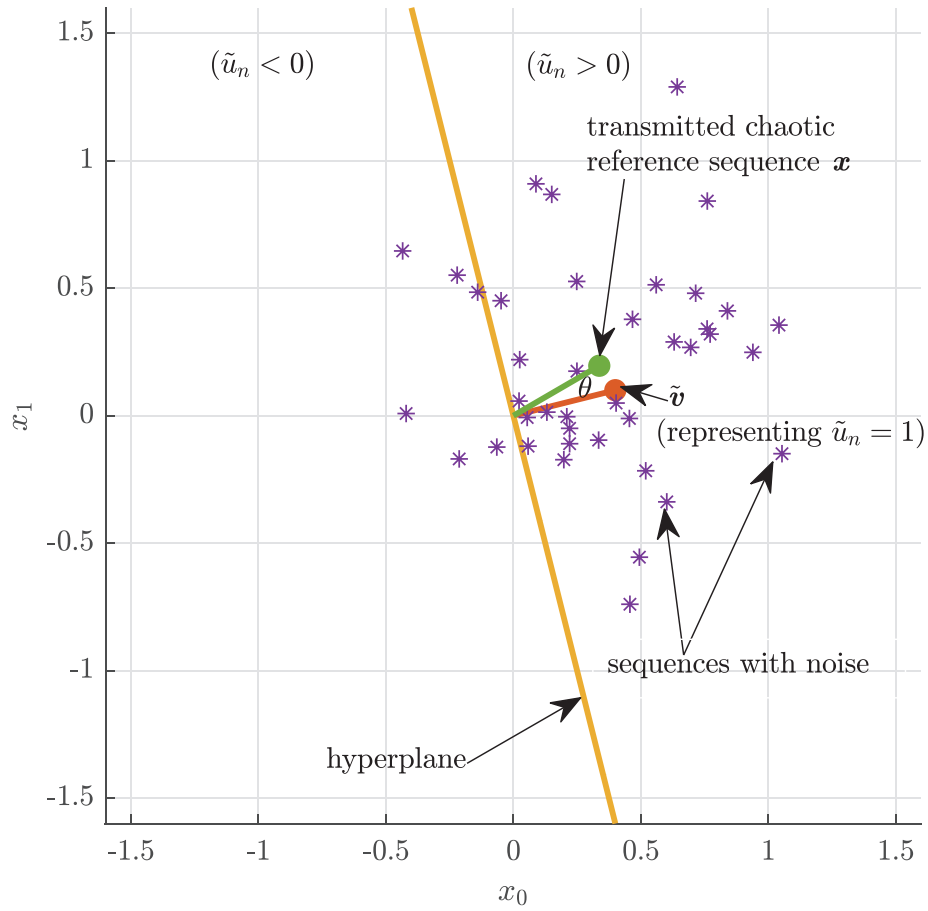


Fig. 3. Illustration of hyperplane over AWGN channel in 2-D space.

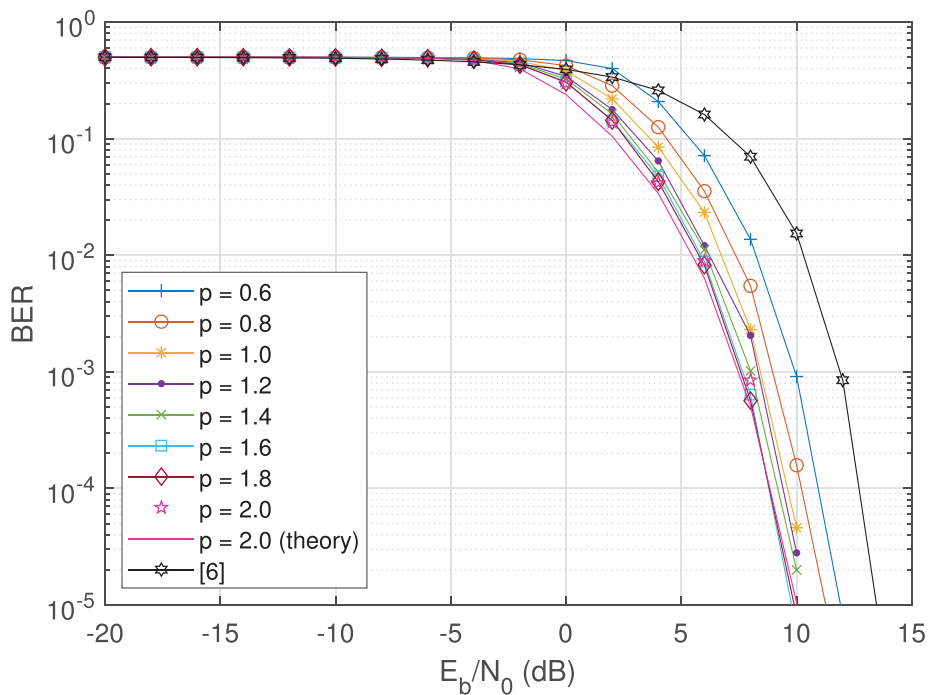


Fig. 4. BER versus E_b/N_0 in AWGN.

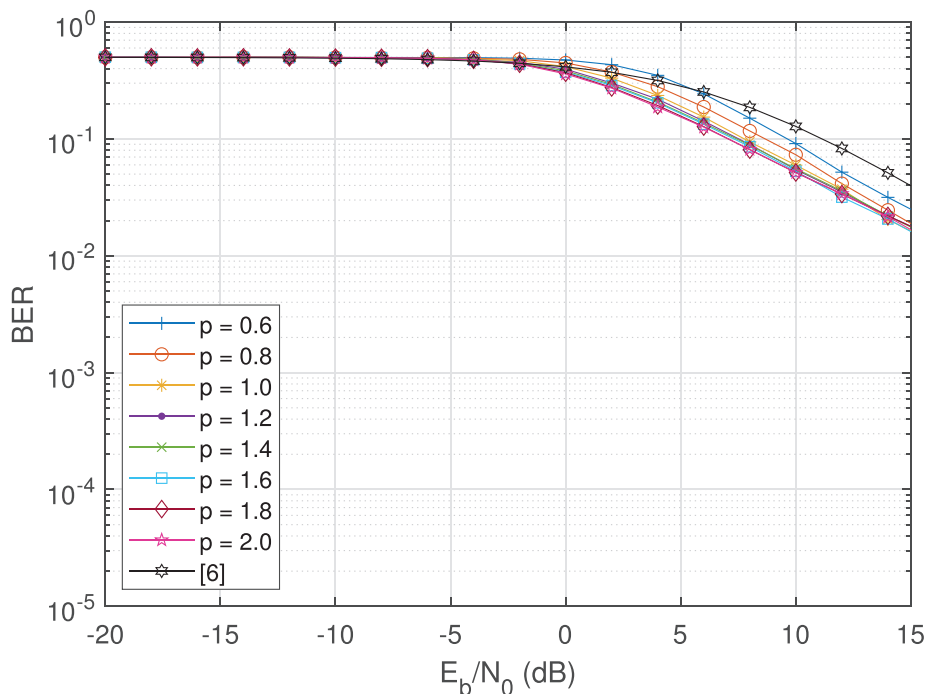


Fig. 5. BER versus E_b/N_0 in AWGN over multipath fading channel.

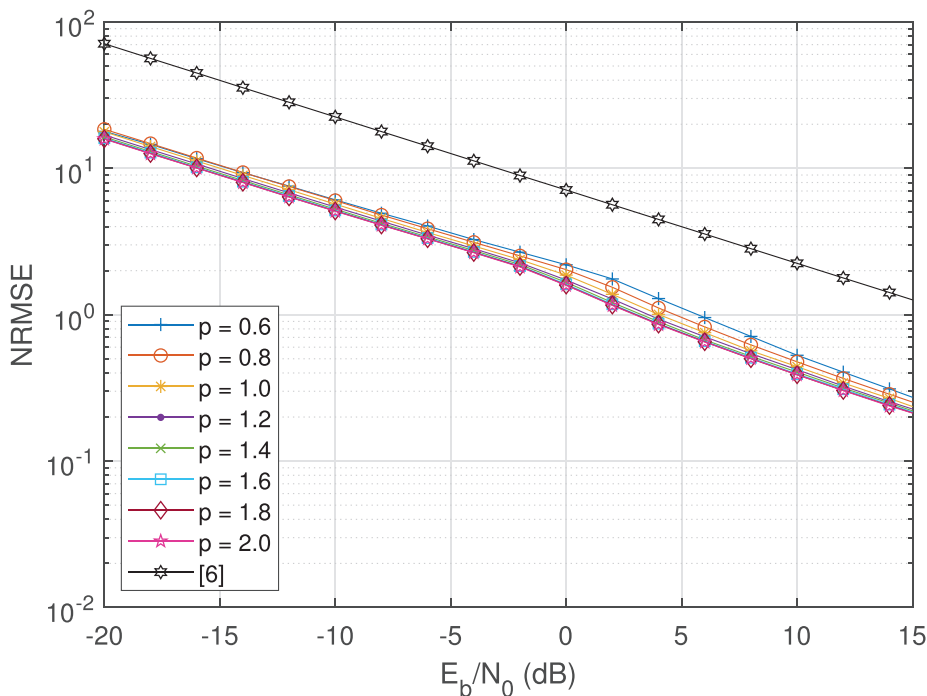


Fig. 6. NRMSE versus E_b/N_0 in AWGN.

(PDF) is expressed as [10]:

$$p(\xi) = e^{-A} \sum_{m=0}^{\infty} \frac{A^m}{m! \sqrt{2\pi\sigma_m^2}} e^{-\frac{\xi^2}{2\sigma_m^2}} \quad (22)$$

where $\sigma_m^2 = \sigma^2(m/A + \Gamma)/(1 + \Gamma)$. The complex-valued noise is generated by combining two independent components with equal power as the real and imaginary parts. According to [10], we set

$A = 0.01$ and $\Gamma = 0.01$, and the results are shown in Figs. 7–9. Again, the superiority of our approach over [6] is demonstrated in both BER and NRMSE. In Fig. 7, we see that the best BER is attained when $p = 1$ and $p = 1.2$, validating that outliers can be effectively suppressed with $p < 2$. Since global convergence is not guaranteed, employing $p < 1$ results in suboptimum performance. Furthermore, the non-robustness of applying the truncated SVD is clearly ob-

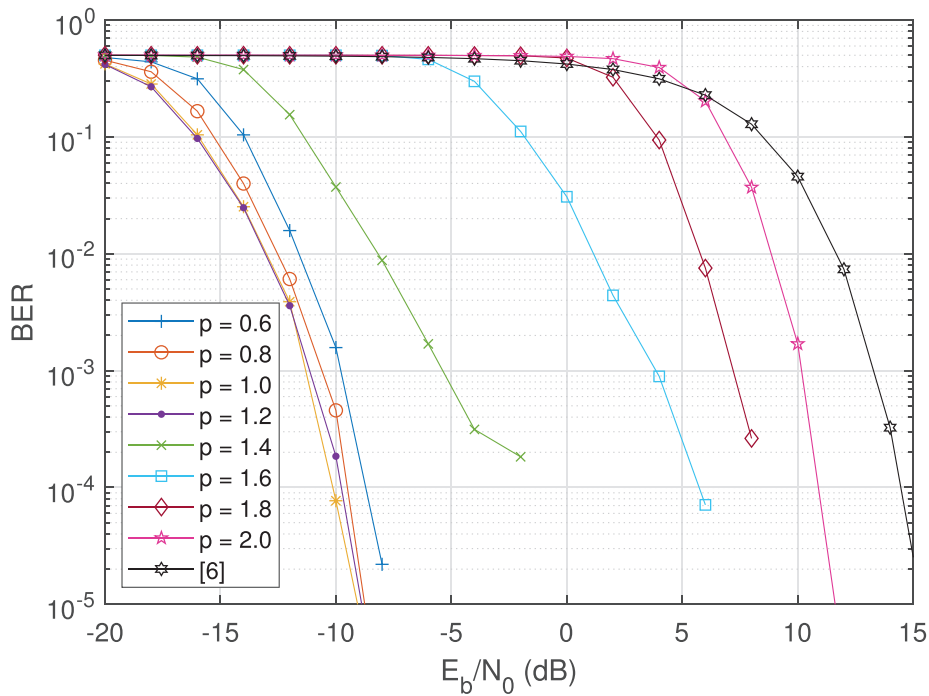


Fig. 7. BER versus E_b/N_0 in Middleton class A noise.

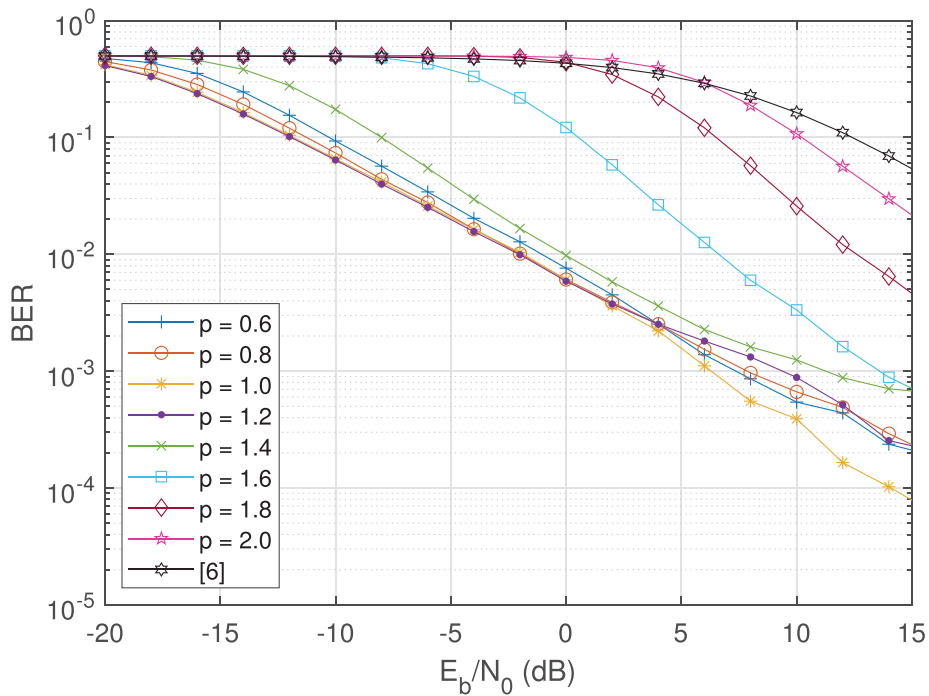


Fig. 8. BER versus E_b/N_0 in Middleton class A noise over multipath fading channel.

served, yielding the worst performance among all choices of p . For multipath fading channel, similar results are obtained. In Fig. 8, the best BER performance is attained with $p = 1$ and $p = 1.2$, and when $p = 2$, the BER performance is the worst since the truncated SVD cannot suppress the impulsive noise well.

Finally, we consider another typical impulsive noise model, namely, zero-location α -stable process, whose PDF is defined as

[25]:

$$p(\xi) = \frac{1}{\pi} \int_0^\infty e^{-\gamma t^\alpha} \cos[\xi t + \gamma \beta_0 t^\alpha \omega(t, \alpha)] dt \tag{23}$$

where α is the characteristic exponent, γ is the scale parameter, β_0 is the symmetry parameter, while $\omega(t, \alpha) = \tan(\alpha\pi/2)$ when $\alpha \neq 1$ and $\omega(t, \alpha) = 2 \log(|t|)/\pi$ when $\alpha = 1$. Because of the undefined variance, we use a generalized form of E_b/N_0 , given by

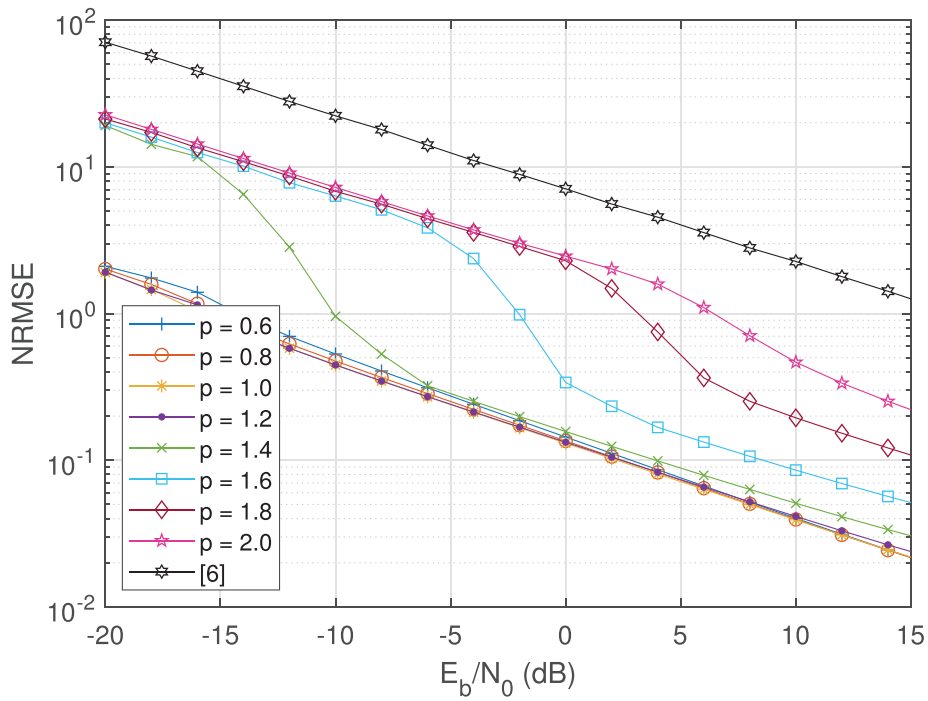


Fig. 9. NRMSE versus E_b/N_0 in Middleton class A noise.

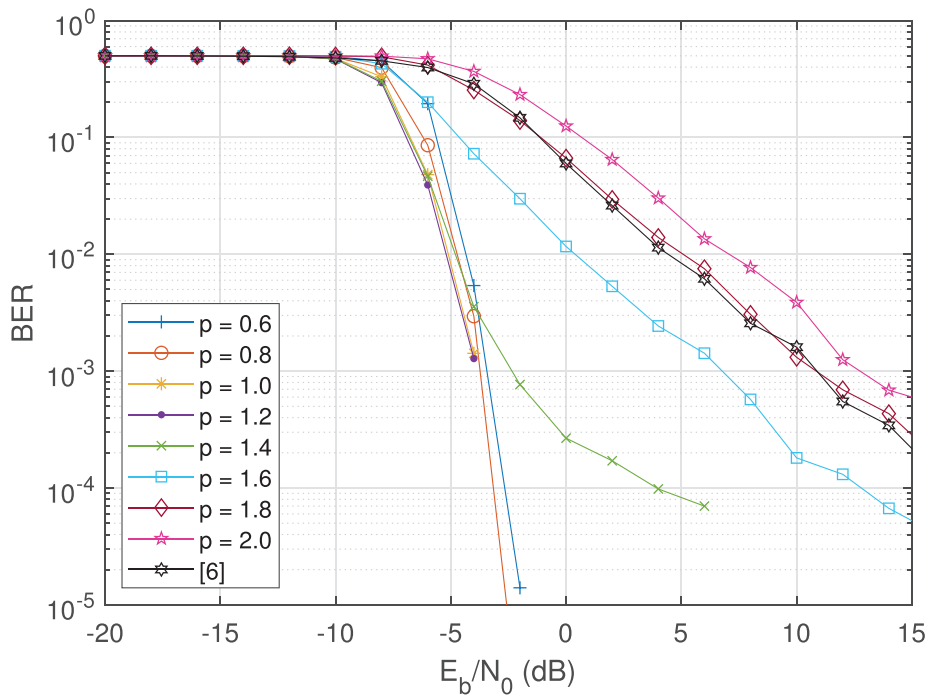


Fig. 10. BER versus E_b/N_0 in α -stable noise.

$E_b/(8\gamma^{2/\alpha})$ [11]. In this test, we fix $\alpha = 1.8$ and vary γ to generate different values of E_b/N_0 . The BER and NRMSE results are plotted in Figs. 10–12. As in Fig. 10, we see that our receiver attains the best BER performance with $p = 1$ and $p = 1.2$, although those of $p = 1.8$ and $p = 2$ are inferior to [6]. Similar results over multipath fading channel can be seen in Fig. 11, where only the case of our proposed scheme with $p = 2$ has the in-

ferior performance comparing with [6]. Nevertheless, the NRMSE of [6] is largest in the whole range of E_b/N_0 . Employing the termination criterion described in Section 2, we have found that when the algorithm is executed by an i7-9700 3.00 GHz CPU and MATLAB parallel computing toolbox, the convergence time is between 0.2 s and 0.6 s, depending on different values of p and E_b/N_0 .

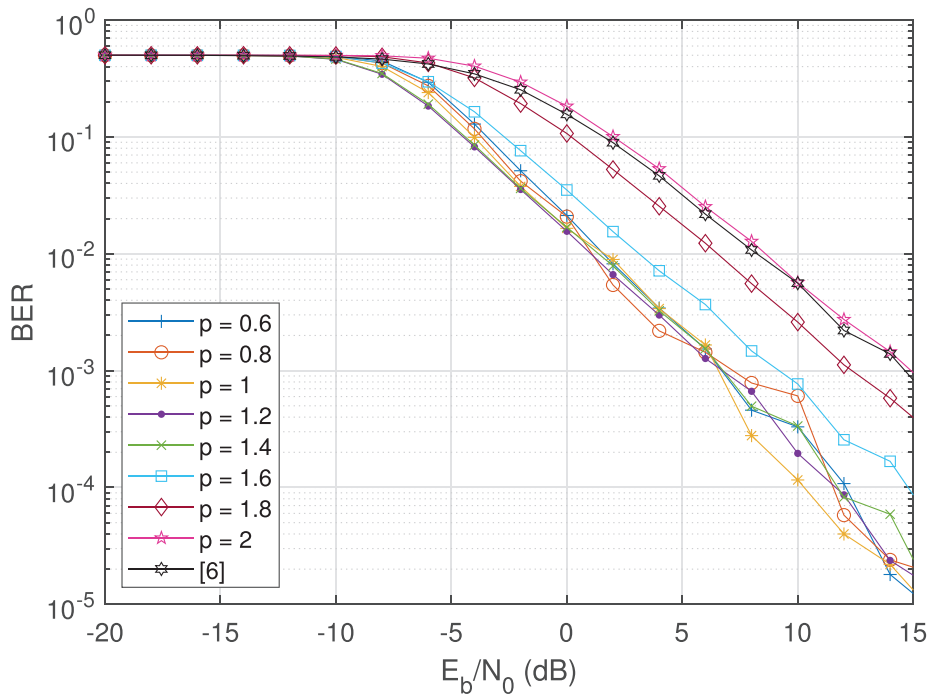


Fig. 11. BER versus E_b/N_0 in α -stable noise over multipath fading channel.

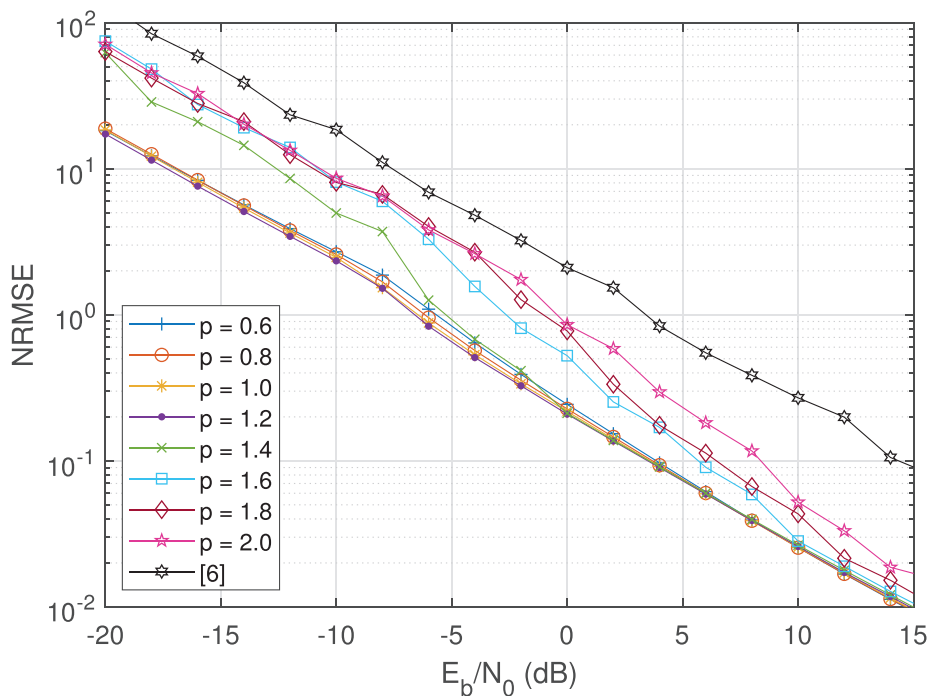


Fig. 12. NRMSE versus E_b/N_0 in α -stable noise.

5. Conclusion

An improved OFDM-DCSK receiver by exploiting the rank-1 property of the symbol matrix has been devised. The rank-1 approximation is attained via matrix factorization and ℓ_p -minimization, resulting in noise suppression. For AWGN, we simply compute the truncated SVD for its realization, which corresponds to $p = 2$. To handle impulsive noise, we set $0 < p < 2$ and apply

the IRLS algorithm to solve the minimization problem. It is demonstrated that the proposed receiver outperforms the conventional scheme for both AWGN as well as impulsive noise models including the Middleton class A noise and α -stable process in terms of BER and NRMSE with a wide range of $p \leq 2$. The error probability for the AWGN case is also derived and verified by computer simulations.

Declaration of Competing Interest

We declare that we have no known competing financial interests or personal relationships that could have appeared to influence the work reported in this paper.

CRediT authorship contribution statement

Zhaofeng Liu: Conceptualization, Methodology, Software, Validation, Formal analysis, Writing - original draft. **Hing Cheung So:** Methodology, Formal analysis, Supervision, Project administration, Writing - review & editing. **Lin Zhang:** Writing - review & editing. **Xiao Peng Li:** Software, Validation.

References

- [1] Y. Fang, G. Han, P. Chen, F.C.M. Lau, G. Chen, L. Wang, A survey on DCSK-based communication systems and their application to UWB scenarios, *Commun. Surv. Tuts.* 18 (3) (2016) 1804–1837.
- [2] G. Kaddoum, N. Tadayon, Differential chaos shift keying: a robust modulation scheme for power-line communications, *IEEE Trans. Circuits Syst. II* 64 (1) (2017) 31–35.
- [3] F.C.M. Lau, C.K. Tse, *Chaos-Based Digital Communication Systems*, Springer, New York, NY, USA, 2003.
- [4] G. Kolumbán, B. Vizvári, W. Schwarz, A. Abel, Differential chaos shift keying: a robust coding for chaos communication, in: *International Workshop on Nonlinear Dynamics of Electronic Systems*, Seville, Spain, 1996, pp. 87–92.
- [5] G. Kaddoum, F.D. Richardson, F. Gagnon, Design and analysis of a multi-carrier differential chaos shift keying communication system, *IEEE Trans. Commun.* 61 (8) (2013) 3281–3291.
- [6] S. Li, Y. Zhao, Z. Wu, Design and analysis of an OFDM-based differential chaos shift keying communication system, *J. Commun.* 10 (3) (2015) 199–205.
- [7] G. Kaddoum, Design and performance analysis of a multiuser OFDM based differential chaos shift keying communication system, *IEEE Trans. Commun.* 64 (1) (2016) 249–260.
- [8] Z. Liu, L. Zhang, Z. Wu, J. Bian, A secure and robust frequency and time diversity aided OFDM-DCSK modulation system not requiring channel state information, *IEEE Trans. Commun.* 68 (3) (2020) 1684–1697.
- [9] Z. Liu, L. Zhang, Z. Wu, Reliable and secure pre-coding OFDM-DCSK design for practical cognitive radio systems with the carrier frequency offset, *IEEE Trans. Cogn. Commun. Netw.* 6 (1) (2020) 189–200.
- [10] K.C. Wiklundh, P.F. Stenumgaard, H.M. Tullberg, Channel capacity of Middleton's class A interference channel, *Electron. Lett.* 45 (24) (2009) 1227–1229.
- [11] G. Laguna-Sanchez, M. Lopez-Guerrero, On the use of alpha-stable distributions in noise modeling for PLC, *IEEE Trans. Power Deliv.* 30 (4) (2015) 1863–1870.
- [12] G. Kaddoum, E. Soujeri, NR-DCSK: a noise reduction differential chaos shift keying system, *IEEE Trans. Circuits Syst. II* 63 (7) (2016) 648–652.
- [13] W. Rao, L. Zhang, Z. Zhang, Z. Wu, Noise-suppressing chaos generator to improve BER for DCSK systems, in: *2017 IEEE International Conference on Communications (ICC)*, Paris, France, 2017, pp. 1–6.
- [14] B. Chen, L. Zhang, Z. Wu, General iterative receiver design for enhanced reliability in multi-carrier differential chaos shift keying systems, *IEEE Trans. Commun.* 67 (11) (2019) 7824–7839.
- [15] M. Miao, L. Wang, G. Chen, W. Xu, Design and analysis of replica piecewise M -ary DCSK scheme for power line communications with asynchronous impulsive noise, *IEEE Trans. Circuits Syst. I* (2020) 1–11.
- [16] G. Zhang, B. Xu, K. Zhang, J. Hou, T. Xie, X. Li, F. Liu, Research on a noise reduction method based on multi-resolution singular value decomposition, *Appl. Sci.* 10 (2020) 1409.
- [17] W.-J. Zeng, H.C. So, Outlier-robust matrix completion via ℓ_p -minimization, *IEEE Trans. Signal Process.* 66 (5) (2018) 1125–1140.
- [18] W.-J. Zeng, H.C. So, L. Huang, ℓ_p -MUSIC: robust direction-of-arrival estimator for impulsive noise environments, *IEEE Trans. Signal Process.* 61 (17) (2013) 4296–4308.
- [19] X.P. Li, Q. Liu, H.C. So, Rank-one matrix approximation with ℓ_p -norm for image inpainting, *IEEE Signal Process. Lett.* 27 (2020) 680–684.
- [20] D.P. O'Leary, Robust regression computation using iteratively reweighted least squares, *SIAM J. Matrix Anal. Appl.* 11 (3) (1990) 466–480.
- [21] R.A. Maronna, R.D. Martin, V.J. Yohai, M. Salibián-Barrera, *Robust Statistics: Theory and Methods* (with R), Wiley Series in Probability and Statistics, Wiley, 2019.
- [22] Y. Xia, C.K. Tse, F.C.M. Lau, Performance of differential chaos-shift-keying digital communication systems over a multipath fading channel with delay spread, *IEEE Trans. Circuits Syst. II* 51 (12) (2004) 680–684.
- [23] M. Barkat, *Signal Detection and Estimation*, Artech House Radar Library, Artech House, 2005.
- [24] D. Middleton, Non-Gaussian noise models in signal processing for telecommunications: new methods and results for class A and class B noise models, *IEEE Trans. Inf. Theory* 45 (4) (1999) 1129–1149.
- [25] C.L. Nikias, M. Shao, *Signal Processing with Alpha-Stable Distributions and Applications*, Wiley-Interscience, USA, 1995.